scientific reports

Check for updates

OPEN

Modulatory effects of 6-Gingerol on erythrocyte deformability and morphology following lower extremity skeletal muscle ischemia-reperfusion injury in rats

Tayfun Özdem[1✉], Hakan Kartal[2], Faruk Metin Çomu[4], Ertan Demirdaş[2], Başak Yavuz[5], Elif Ertaş[6], Gökhan Erol[2], Tuna Demirkıran[1], Şahin Kaymak[3], Muharrem Emre Özdaş[7], Işıl Taşöz Özdaş[1], Yigit Tokgöz[2] & Veli Can Özdemir[2]

Oxidative stress from ischemia-reperfusion (IR) injury severely compromises erythrocyte deformability, a critical factor that disrupts microvascular flow and thereby exacerbates reperfusion injury. This study provides a novel perspective by directly investigating the protective effects of 6-Gingerol, known for its potent antioxidant properties, on erythrocyte function in a rat model of lower-extremity skeletal muscle IR. Twenty-four Wistar albino rats were divided into four groups: Sham ($n = 6$), DMSO ($n = 6$), IR ($n = 6$), and 6-Gingerol-IR (6G-IR, $n = 6$, 6 mg/kg i.p., 1 h before ischemia). Ninety minutes of ischemia were followed by 90 min of reperfusion. Compared to the IR group, the 6G-IR group exhibited a significant improvement in erythrocyte deformability (Rrel 2.13 ± 0.36 vs. 3.29 ± 0.40; $p = 0.002$, Cohen's d = 3.9), a substantial reduction in lipid peroxidation (MDA 16.23 ± 2.11 vs. 22.14 ± 5.78 nmol/ml; $p = 0.002$, Cohen's d = 1.3), and an apparent increase in antioxidant capacity (SOD 11.36 ± 2.25 vs. 6.93 ± 2.54 U/ml; $p < 0.001$, Cohen's d = 2.0). Furthermore, 6G-IR significantly attenuated morphological damage (MGG score) and suppressed eNOS expression (H-score) compared to the IR group (Cohen's d = 1.7 and d = 1.4, respectively). These findings provide strong preliminary evidence that 6-Gingerol preserves microcirculatory function through SOD-mediated neutralization of superoxide, thereby preventing peroxynitrite-induced erythrocyte membrane damage. Further power-calculated studies are warranted to explore its clinical translational potential.

Keywords 6-Gingerol, Ischemia/reperfusion, Erythrocyte, Deformability, ENOS

Ischemia-reperfusion (IR) injury is a paradoxical tissue damage that occurs when blood flow is restored to tissues that were previously deprived of blood and oxygen. This complex pathological process has been the focus of extensive basic and clinical research for years. Cellular damage during ischemia is worsened by reperfusion, which triggers mechanisms such as oxidative stress and inflammation. This can lead to cell death and tissue dysfunction. IR injury plays a key role in various clinical conditions, including myocardial infarction, stroke, organ transplantation, and trauma[1].

Unsaturated fatty acids in cell membranes are highly vulnerable to damage caused by free radicals. This damage can disrupt the structure and function of the cell membrane, resulting in loss of function[2].

For erythrocytes to pass successfully through microcirculation, especially through capillaries that are smaller in diameter than the cells, it is crucial that they have a high degree of deformability. This deformability comes from the viscoelastic properties of the erythrocyte membrane, which enable the cell to squeeze through narrow

[1]Ministry of Health Gulhane Education and Research Hospital , Ankara 06000, Turkey. [2]Department of Cardiovascular Surgery , Gulhane Education and Research Hospital, University of Health Sciences , Ankara 06000, Turkey. [3]Department of General Surgery , Gulhane Education and Research Hospital, University of Health Sciences , Ankara 06000, Turkey. [4]Department of Physiology, Faculty of Medicine , Kirikkale University , Kırıkkale 71000, Turkey. [5]Department of Histology and Embryology Faculty of Medicine , Izmir Democracy University , Izmir 35000, Turkey. [6]Department of Biostatistics , Selçuk University , Konya 42000, Turkey. [7]Department of Pediatric Cardiovascular Surgery , Etlik City Hospital , Ankara 06000, Turkey. ✉email: tayfunozdem@yahoo.com

capillaries and then return to its original shape. The shape memory of the erythrocyte membrane is vital for maintaining its biconcave disc shape and functionality despite repeated deformation cycles. Any impairment in its ability to deform may hinder erythrocytes from passing through capillaries, resulting in microcirculatory problems[3]. Decreased erythrocyte deformability is a key indicator in many diseases, including IR injury, diabetes, and sepsis[3,4]. The significance of these mechanical changes under pathological and even blood storage conditions continues to be the focus of ongoing research[5].

When oxidative stress and inflammation rise, the deformability of erythrocytes declines. This condition decreases blood fluidity, adversely impacting microcirculation and potentially advancing related diseases[3,6].

6-Gingerol is one of the main active compounds extracted from the rhizome of Zingiber officinale, a plant in the Zingiberaceae family. It is known for its anti-inflammatory and antioxidant properties[7]. Notably, the anti-inflammatory and antioxidant capacity of gingerols on immune cells has recently been a topic of interest[8]. Although its systemic benefits are well documented, few studies have examined its specific effects on erythrocyte physiology under oxidative stress. Because erythrocyte membranes are prone to lipid peroxidation and redox imbalance, we hypothesized that 6-Gingerol helps maintain erythrocyte deformability and shape during IR injury by reducing oxidative damage.

Despite extensive research into 6-Gingerol's cardioprotective and neuroprotective effects following IR, its specific role in preserving the rheological function of circulating erythrocytes—a critical determinant of microvascular patency—remains an important, unaddressed knowledge gap. Direct evaluation of erythrocyte deformability provides a mechanistic bridge linking 6-Gingerol's antioxidant properties to improved microcirculatory outcomes.

This study aimed to investigate the protective effects of 6-Gingerol, which possesses antioxidant and anti-inflammatory properties, on erythrocytes in a lower extremity skeletal muscle IR model-induced erythrocyte damage.

Materials and methods

Ethical considerations and chemicals

This study was approved by the Local Ethics Committee of the ***Kobay*** Experimental Animals Laboratory in Ankara, Turkiye, on 08.12.2023 (Approval No: 690). A total of 24 rats were approved for the main study. All experimental procedures were carried out in the same laboratory following the ethics committee's approval. This study is reported in accordance with the ARRIVE guidelines (https://arriveguidelines.org). All efforts were made to minimize animal suffering and to reduce the number of animals used in line with the 3Rs principles (Replacement, Reduction, Refinement). Meticulous monitoring and post-operative pain management were maintained throughout the study period.

The 6-Gingerol used in this study was obtained from Sigma-Aldrich (Sigma-Aldrich, St. Louis, MO, USA; CAS No. 23513-14-6, Purity ≥ 98%). The researchers supplied all reagents and materials, and no external funding sources supported this study.

Sample size determination

In the assessment of mean differences in Malondialdehyde (MDA), Superoxide Dismutase (SOD), Endothelial Nitric Oxide Synthase (eNOS), May-Grunwald-Giemsa (MGG) staining, and Deformability measurements across the Sham, Dimethyl Sulfoxide (DMSO), IR, and 6G-IR (6-Gingerol + IR) treatment groups, the Resource Equation Method (Mead's Rule) was used to determine the required number of rats for animal experiments[9]. This method was chosen as an appropriate approach for this exploratory study where the effect size was unknown a priori, prioritizing the reduction and refinement of animal usage while ensuring adequate degrees of freedom ($E = N - T = 24 - 4 = 20 > 10$) for robust statistical analysis.

Determination of 6-Gingerol dosage and administration

A literature review showed that different doses and methods of giving 6-Gingerol (intravenous, intraperitoneal, oral gavage) have been used. Based on common data, an intravenous (i.v.) dose of 6 mg/kg was first tested; however, giving 6-Gingerol dissolved in DMSO at this dose caused death within five minutes in rats, even though it was below the reported toxic level[10–13]. A later trial with 3 mg/kg i.v. also resulted in death, this time within 10 min, raising doubts about the safety of previous dose recommendations. These initial dose trials were approved under the same institutional ethics approval as the main study. The rapid mortality observed was characterized by sudden cardiovascular collapse, likely due to the rapid bolus delivery of the high concentration of the lipophilic compound and DMSO. These pilot toxicity observations were considered an expected finding in the dose-finding phase when using the i.v. bolus route. After reviewing the literature again, the intraperitoneal (i.p.) administration at 6 mg/kg was chosen. In this case, the rats stayed stable in their blood pressure and heart rate throughout the 3-hour experiment, suggesting that intraperitoneal delivery was prioritized over intravenous bolus administration due to the observed cardiovascular instability and might be the best method for future studies[13,14]. Crucially, no additional animals were allocated for these dose-finding trials beyond the initial animals reported here, adhering strictly to the 3Rs principles.

Animals and experimental procedure

In this study, 24 adult male Wistar albino rats, each weighing between 400 and 450 g, were used. All rats in this study were obtained from Kobay Experimental Animals Laboratory. The subjects were housed in standard cages under controlled conditions of 50% humidity and temperatures ranging from 21 to 24 °C. An adaptation period of 7 days was provided, with three rats housed per cage. The cages maintained a 12-hour light/dark cycle automatically. Throughout the study, all subjects had free access to standard rodent feed and fresh drinking water.

Following the selection of the 6 mg/kg i.p. dose for the main study, all animals ($n = 24$) successfully completed the 3-hour experimental protocol without any mortality.

Before all surgical procedures, anesthesia was administered via intramuscular injection of ketamine hydrochloride (100 mg/kg) and xylazine hydrochloride (10 mg/kg). Core body temperature was maintained within the physiological range throughout the experiment. Following an inguinal incision, a 26-gauge venous cannula was inserted into the femoral vein, and all groups received intravenous heparin (100 U/kg). To avoid potential confounding effects, the same heparin dose was administered across all groups.

The rats were randomly assigned to four groups, with each group consisting of six rats. Animals were randomized into groups using a computer-generated randomization list:

Group Sham: In this group of rats, only an incision was made in the inguinal region under anesthesia, and then it was closed. Intracardiac blood sampling was performed three hours later.

Group DMSO: To assess the potential effects of DMSO on erythrocytes, the same amount of DMSO was administered intraperitoneally as in the 6-Gingerol-treated groups (1 ml of DMSO dissolves up to 25 mg of 6-Gingerol[15]. Under anesthesia, an incision was made in the inguinal region, which was then closed, and intracardiac blood sampling was performed three hours later. Ischemia was not induced.

Group IR: In this group of rats, under anesthesia, the femoral artery was accessed through the inguinal region, and a gentle microvascular clamp was applied for 90 min to induce ischemia. After this period, the clamp was removed, and reperfusion was maintained for 90 min. Intracardiac blood sampling was performed after the procedure.

Group 6G-IR: In this study, 6 mg/kg of 6-Gingerol was administered intraperitoneally one hour before inducing IR injury. Then, under anesthesia, the femoral artery was accessed via the inguinal region, and an atraumatic microvascular clamp was applied for 90 min to induce ischemia. The clamp was then removed, and reperfusion was maintained for 90 min. Afterward, intracardiac blood sampling was performed.

From the collected blood samples, two peripheral blood smears were prepared. The first smear was air-dried for MGG staining, then numbered and stored. The second smear was fixed in 98% pure ethanol for 30 min for eNOS immunohistochemical staining, then numbered and stored. For erythrocyte deformability analyses, blood samples were collected in heparin-coated blood gas syringes, numbered, and stored at + 4 °C. To determine SOD and MDA levels, blood samples were centrifuged at 3000 rpm for 15 min, plasma was separated, numbered, and stored at −80 °C.

Deformability measurements

To prevent hemolysis, blood samples were carefully collected, and the measurement process was performed as quickly as possible. Hemolysis was excluded in all samples by visual inspection prior to analysis. The collected blood was centrifuged at 1,000×g for 10 min. The serum and buffy coat were removed, and isotonic phosphate-buffered saline (PBS) was added to the erythrocyte pellet, followed by centrifugation at 1,000×g for 10 min. This washing process was repeated three times to obtain purified erythrocyte preparations. The erythrocytes were then resuspended in PBS to achieve a hematocrit of 5%, and all deformability measurements were standardized to this hematocrit to eliminate viscosity-related confounding. All measurements were initiated within 30 min of blood collection and performed at a controlled temperature of 22 °C.

Erythrocyte deformability was assessed using a constant-flow filtrometry system. Samples were prepared as a 10 mL erythrocyte suspension in PBS buffer and perfused through a nucleoporin polycarbonate filter (pore diameter: 5 µm; diameter: 28 mm) at a constant flow rate of 1.5 mL/min using an infusion pump. Pressure changes generated during filtration were detected by a pressure transducer and recorded via an MP30 data acquisition system (BIOPAC Systems Inc., Goleta, CA). System pressure calibration was performed before each measurement. Buffer-only filtration was conducted first, followed by erythrocyte suspension filtration, and pressure values were recorded accordingly.

The relative resistance (Rrel) was calculated as the ratio of the pressure generated by the erythrocyte suspension to that of the buffer alone. An increase in Rrel was interpreted as a decrease in erythrocyte deformability[16,17].

Histological evaluation and morphometry

For the histopathological examination, peripheral blood smears were stained with MGG stain and examined under a light microscope. While the erythrocytes in the Sham group displayed normal morphology, the IR group showed morphological abnormalities such as echinocytes, dacrocytosis, and rouleaux formation. These changes were semi-quantitatively scored in MGG-stained preparations. A blinded scoring system was used independently by two researchers, rating on a scale from 0 to 5 (1: none/minimal; 2: mild; 3: moderate; 4: significant; 5: severe)[18–20]. Both histological scoring and immunohistochemical evaluations were performed under blinded conditions by personnel unaware of the group assignments. Although formal inter-observer agreement statistics (e.g., Kappa or ICC) were not calculated, a high degree of qualitative concordance was observed between the two observers for the MGG scoring.

Immunohistochemical evaluation and H-score

In this study, eNOS expressions in peripheral blood smears were assessed using the indirect immunohistochemistry method. The smears, fixed with 98% ethanol, were incubated in a Twin Buffer Solution (TBST, pH 7.4) for 15 min, followed by washing with TBST. To prevent nonspecific binding, the smears were incubated for 30 min with 1% hydrogen peroxide (Lab Vision, Thermo Scientific, Fremont, USA).

As the primary antibody, a 1:100 dilution of eNOS antibody (Boster Bio PA2140-2) was used. The peripheral blood smears were incubated overnight at + 4 °C. Then, the samples were incubated at room temperature for 20 min with a biotinylated secondary antibody (Lab Vision, Thermo Scientific), followed by another 20-minute

incubation with streptavidin peroxidase enzyme (Lab Vision, Thermo Scientific). After each incubation, the peripheral blood smears were washed with TBST.

To develop the color reaction, the slides were incubated with diaminobenzidine chromogen substrate for 5–10 min at room temperature. Contrast staining was performed using Mayer's hematoxylin. The eNOS immunoreactivity was assessed using the H-score method on the obtained images.

In indirect immunohistochemical staining, moderate eNOS expression was observed in erythrocytes, which increased with IR. Semi-quantitative results of immunohistochemical staining were analyzed using the H-score method. For this purpose, staining intensities were scored as weak (1), moderate (2), and strong (3), and the number of stained cells was counted in three different microscopic fields for each intensity. The data obtained were calculated using the formula H-score = ∑[Percentage of stained cells (Pi) × (Staining Intensity + 1)]. This formula is a common adaptation in semi-quantitative scoring, designed to give greater weight to stronger staining intensities. In this formula, Pi refers to the percentage of cells labeled for density, ranging from 0% to 100%[18]. Scoring was performed independently by two blinded observers. A high degree of qualitative agreement was established between the two observers for the H-score assessment. It is important to note that immunohistochemical staining in this study reflects the qualitative expression levels of the eNOS protein but does not provide quantitative data on its catalytic activity or functional nitric oxide (NO) bioavailability.

Biochemical analysis

In this study, SOD and MDA levels were measured quantitatively using the ELISA technique. Blood samples were coded, and all biochemical analyses were carried out under strict blinded conditions by personnel unaware of the treatment group to eliminate observer bias.

SOD Analysis: For measuring SOD levels, a commercial ELISA kit (SunRed Biological Technology Co. Ltd., Cat No. 201-11-0169, Shanghai, China, Ref: DZE201110169, Lot: 202311) was used. According to the kit protocol, all reagents were brought to room temperature and diluted accordingly. SOD standards were prepared at concentrations of 64 ng/ml, 32 ng/ml, 16 ng/ml, 8 ng/ml, 4 ng/ml, and 2 ng/ml from the stock standard solution. 50 µl of each standard solution was pipetted into the respective wells. Since the standard solution contained a biotin-labeled antibody, no additional antibody was added to the standard wells. Samples were added to the wells in 40 µl volumes, followed by 10 µl of anti-SOD antibody for incubation. 50 µl of streptavidin-HRP was added to both the standard and sample wells, and the plate was incubated at 37 °C for 60 min. After incubation, the wells were washed five times with 350 µl of washing solution using an ELISA washer. Then, 50 µl of Chromogen A and 50 µl of Chromogen B were added to each well. After incubating the plate in the dark at 37 °C for 10 min, the reaction was stopped by adding 50 µl of stop solution to each well, causing a color change from blue to yellow. The absorbance was measured at 450 nm within 15 min using a microplate reader.

MDA Analysis: To determine MDA levels, a commercial ELISA kit (SunRed Biological Technology Co. Ltd., Cat No. 201-11-0157, Shanghai, China, Ref: DZE201110157, Lot: 202311) was used. According to the kit protocol, all reagents were diluted at room temperature. MDA standards were prepared at concentrations of 40 ng/ml, 20 ng/ml, 10 ng/ml, 5 ng/ml, 2.5 ng/ml, and 1.25 ng/ml from the stock standard solution. 50 µl of each standard solution was pipetted into the respective wells. Since the standard solution contained a biotin-labeled antibody, no additional antibody was added to the standard wells. Samples were added to the wells in 40 µl volumes, followed by 10 µl of anti-MDA antibody for incubation. 50 µl of streptavidin-HRP was added to both the standard and sample wells, and the plate was incubated at 37 °C for 60 min. After incubation, the wells were washed five times with 350 µl of washing solution using an ELISA washer. Next, 50 µl of Chromogen A and 50 µl of Chromogen B solutions were added to each well. After the plate was incubated in the dark at 37 °C for 10 min, the reaction was stopped by adding 50 µl of stop solution to each well, causing a color change from blue to yellow. The absorbance was then measured at 450 nm using a microplate reader within 15 min.

Statistical analysis

For the statistical analysis of continuous data, mean and standard deviation values were provided. The normality of distribution for all measured parameters was first evaluated using the Shapiro-Wilk test, and all data sets were confirmed to follow a normal distribution. In the treatment groups, One-Way ANOVA test statistics were used to compare the means of continuous measurements such as Deformability, MGG, MDA, eNOS, and SOD. When a significant difference was detected, pairwise comparisons were performed using the Post Hoc Tukey test. Results are presented with exact p-values where possible, and ANOVA results include F-values and degrees of freedom (F(df, df)). The level of statistical significance was set at $p < 0.05$. IBM SPSS 25 statistical software was used for data analysis.

Results

Erythrocyte deformability and morphological findings

The erythrocyte deformability index (Rrel) was significantly impaired in the IR group compared to the Sham group ($F(3, 20) = 45.18$, $p < 0.001$). Pre-treatment with 6-Gingerol significantly preserved erythrocyte deformability in the 6G-IR group compared to the IR group (Rrel 2.13 ± 0.36 vs. 3.29 ± 0.40; $p = 0.002$). The DMSO group showed no significant difference from the Sham group (Rrel 1.89 ± 0.28 vs. 1.78 ± 0.21; $p = 0.542$).

The MGG staining showed that the IR group had significantly higher erythrocyte morphological damage scores than the Sham group ($F(3, 20) = 28.35$, $p = 0.001$). The 6G-IR group had significantly lower morphological damage scores compared to the IR group. Specifically, the MGG score decreased from 4.17 ± 0.41 in the IR group to 3.00 ± 0.00 in the 6G-IR group ($p = 0.003$, Cohen's $d = 1.7$). The DMSO group did not differ significantly from the Sham group Fig. 1.

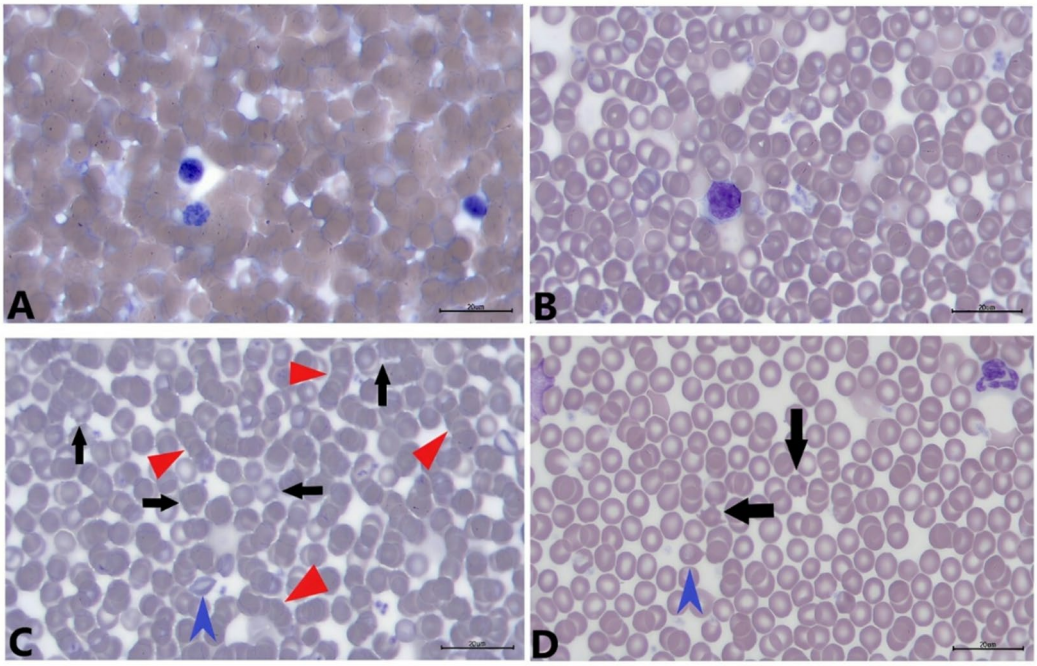

Fig. 1. These may-grunwald-giemsa-stained photographs of the experimental groups sham, dimethyl sulfoxide, ischemia-reperfusion (IR), and 6-Gingerol + IR can be seen in (**A**, **B**, **C**, and **D**) respectively. Black arrows show echinocytes, blue arrowheads show dacrocytes, and red arrowheads show Rouloux formation.

Biochemical markers of oxidative stress (SOD and MDA)

The MDA levels, an indicator of lipid peroxidation, were significantly increased in the IR group compared to the Sham group ($F(3, 20) = 19.42$, $p = 0.002$). The 6G-IR group demonstrated a significant reduction in MDA levels compared to the IR group (16.23 ± 2.11 nmol/ml vs. 22.14 ± 5.78 nmol/ml; $p = 0.002$, Cohen's $d = 1.3$).

SOD activity, an essential endogenous antioxidant enzyme, was significantly decreased in the IR group compared to the Sham group ($F(3, 20) = 25.10$, $p < 0.001$). The 6G-IR group showed a significant increase in SOD levels compared to the IR group (11.36 ± 2.25 U/ml vs. 6.93 ± 2.54 U/ml; $p < 0.001$, Cohen's $d = 2.0$). No significant difference was observed between the Sham and DMSO groups for both MDA and SOD levels.

Immunohistochemical findings (eNOS)

The eNOS expression (H-score) was significantly elevated in the IR group compared to the Sham group ($F(3, 20) = 17.65$, $p = 0.003$). The 6G-IR group showed a significant decrease in eNOS expression compared to the IR group. The H-score decreased from 3.76 ± 0.49 in the IR group to 2.87 ± 0.31 in the 6G-IR group ($p = 0.003$, Cohen's $d = 1.4$). The DMSO group did not show a significant change compared to the Sham group Fig. 2.

Summary of statistical comparison

A comprehensive summary of the mean ± SD values and ANOVA results for all measured parameters is presented in Table 1. This table details the statistical differences between all four groups for Deformability (Rrel), MGG Score, MDA, SOD, and eNOS H-score.

Discussion

Ischemia-reperfusion (IR) injury severely compromises microvascular function, a pathology directly exacerbated by the loss of erythrocyte deformability. Our principal finding is that prophylactic administration of 6-Gingerol significantly ameliorated the IR-induced reduction in erythrocyte deformability and morphological damage in a rat skeletal muscle model. This protective effect highlights 6-Gingerol's potential to improve microcirculatory outcomes, which is critical for tissue survival after reperfusion.

Erythrocytes are highly susceptible to oxidative attack due to their high polyunsaturated fatty acid content, making their membranes vulnerable to lipid peroxidation[27]. IR injury generates vast amounts of reactive oxygen species (ROS), particularly superoxide, leading to massive lipid peroxidation and subsequent membrane rigidification[21]. Our biochemical data directly support this link: the IR group showed a significant increase in malondialdehyde (MDA) levels and a concomitant decrease in superoxide dismutase (SOD) activity. The observed impairment of deformability (increased Rrel) and morphological deterioration (echinocyte formation) in the IR group is a direct consequence of this overwhelming oxidative burden and diminished antioxidant reserve.

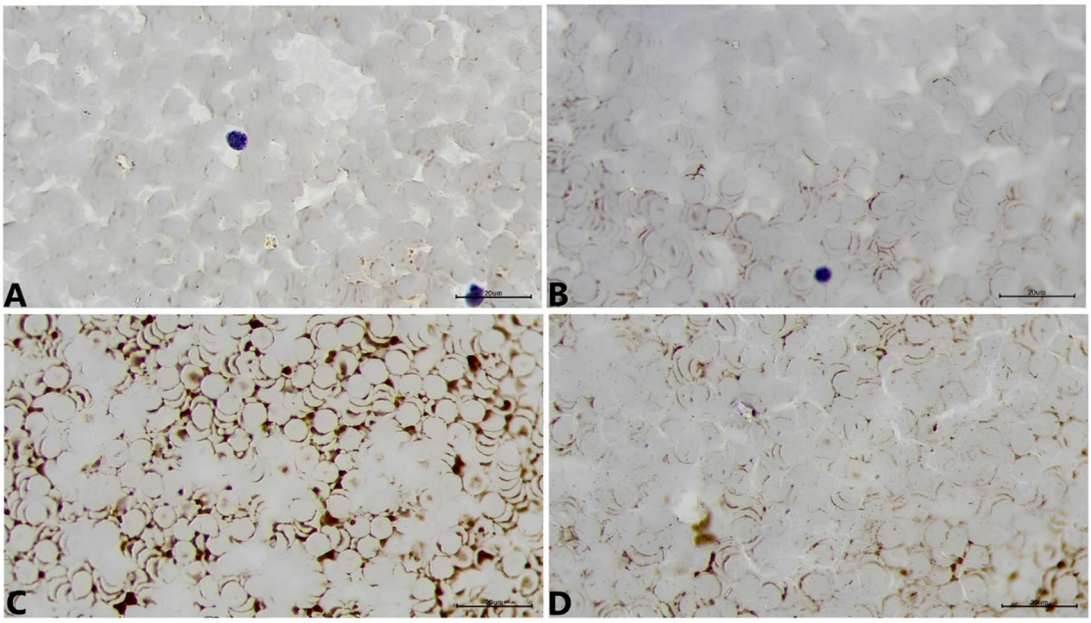

Fig. 2. Immunohistochemical-stained (eNOS stained) photographs of the experimental groups sham, DMSO, IR and 6G-IR can be seen in (**A**, **B**, **C**, and **D**) respectively.

Groups	Deformability(Rrel) mean ± SD	MGG mean ± SD	MDA(nmol/ml) mean ± SD	eNOS (H-score) mean ± SD	SOD(U/ml) mean ± SD
Sham (a)	1.74 ± 0.12^{c}	$2.18 \pm 0.33^{c, d}$	15.56 ± 2.03^{c}	$1.78 \pm 0.21^{c, d}$	4.75 ± 2.57^{d}
DMSO (b)	1.92 ± 0.17^{c}	$2.62 \pm 0.55^{c, d}$	13.91 ± 1.84^{c}	$1.95 \pm 0.25^{c, d}$	5.96 ± 2.72^{d}
IR (c)	$3.29 \pm 0.40^{a, b,d}$	4.17 ± 0.41^{d}	$22.14 \pm 5.78^{a, b,d}$	$3.76 \pm 0.49^{a, b,d}$	6.93 ± 2.54^{d}
6G-IR (d)	2.13 ± 0.36^{c}	$3.00 \pm 0.00^{a, b,c}$	16.23 ± 2.11^{c}	$2.87 \pm 0.31^{a, b,c}$	$11.36 \pm 2.25^{a, b,c}$

Table 1. Comparison of deformability, MGG, MDA, eNOS, SOD measurement values by group type. Values are presented as mean ± standard deviation (SD). Statistical analysis was performed using One-Way ANOVA (with F-values and degrees of freedom reported in the Results section), followed by the Post Hoc Tukey test for pairwise comparisons. Effect sizes (Cohen's d) for critical comparisons are detailed in the relevant Results subsections (3.1, 3.2, and 3.3). $p < 0.05$ was considered statistically significant. Superscript letters (a, b, c, d) indicate significant differences ($p < 0.05$) compared to the respective group. For example, 3.29 ± 0.40a, b, d means the IR group is significantly different from Sham (a), DMSO (b), and 6G-IR (d) groups.

6-Gingerol's protective mechanism: antioxidant and anti-peroxynitrite activity

The core finding of this study demonstrates that 6-Gingerol significantly restored SOD activity and reduced MDA levels, effectively mitigating the effects of oxidative stress. This suggests that 6-Gingerol acts primarily by bolstering the erythrocyte's natural defenses against superoxide radicals. This is particularly important because superoxide, when combined with NO, rapidly forms the highly potent cytotoxic agent peroxynitrite[22,23]. Peroxynitrite is a known driver of erythrocyte membrane damage, exacerbating lipid peroxidation and reducing deformability[23,24]. By increasing SOD activity, 6-Gingerol reduces the availability of superoxide, thereby preventing the formation of peroxynitrite. This proposed mechanism linking 6-Gingerol, SOD activity, and the prevention of peroxynitrite-induced membrane damage is conceptually summarized in Fig. 3.

Interpretation of eNOS results

The immunohistochemical results showed a significant increase in eNOS H-score in the IR group, which was significantly suppressed by 6-Gingerol treatment. While eNOS is primarily viewed as a protective enzyme, its expression and functional outcome are complex in IR settings. The presence and functional relevance of eNOS in erythrocytes remain a subject of ongoing debate; accordingly, the present findings should be interpreted as alterations in immunoreactivity rather than definitive evidence of enzymatic activity or nitric oxide bioavailability. The increase in eNOS expression in the IR group may reflect a compensatory physiological attempt by erythrocytes to generate more NO in response to elevated oxidative stress and microvascular dysfunction. However, in an environment saturated with superoxide, this increased NO availability is rapidly diverted toward the formation of damaging peroxynitrite. Our conclusion regarding eNOS must be tempered by acknowledging the limitations of immunostaining alone. While the reduction in eNOS H-score in the 6G-IR

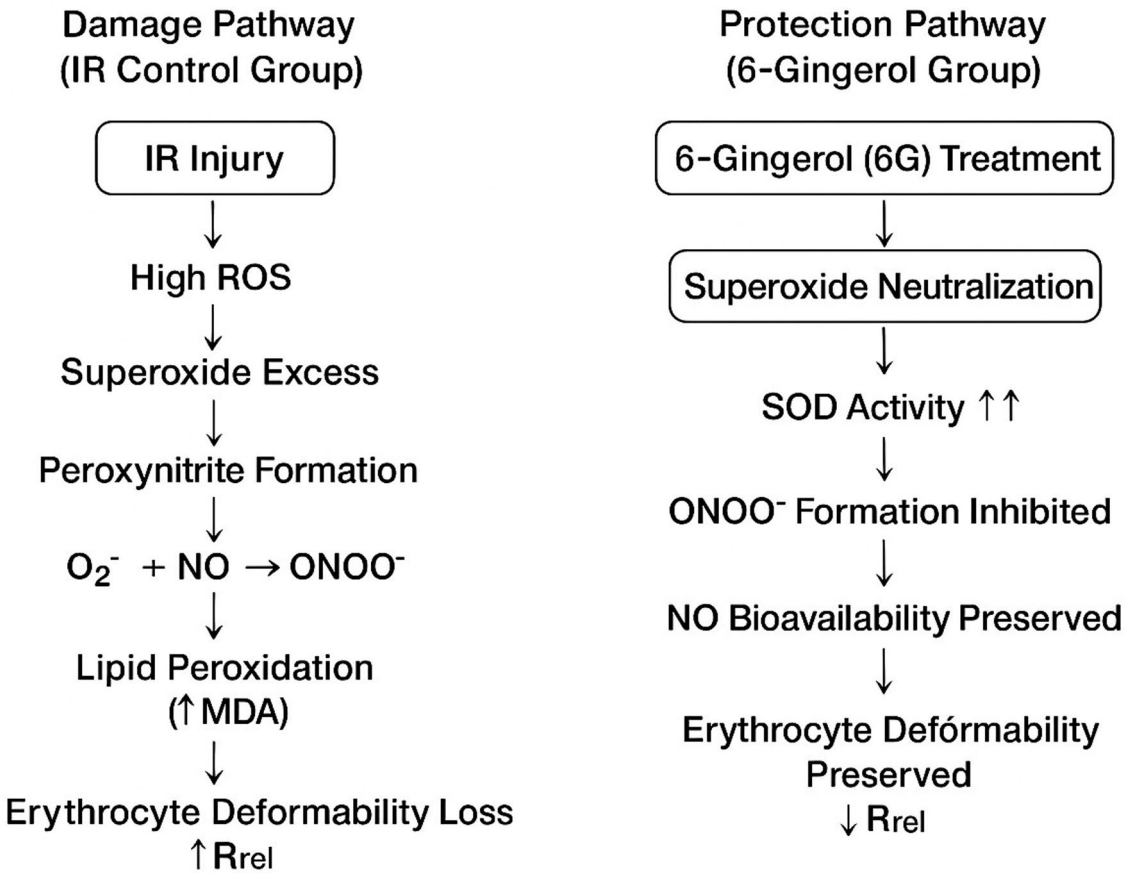

Fig. 3. Proposed mechanistic pathway of 6-Gingerol protection against ischemia-reperfusion-induced erythrocyte dysfunction.

group suggests a reduction in the pathological stress that initially triggered its upregulation, this finding does not provide functional insight into NO bioavailability. Further studies measuring NO metabolites (nitrite/nitrate) and peroxynitrite-specific markers (e.g., nitrotyrosine) are required to definitively establish the functional state of the NO signaling pathway in these cells[25,26].

Therole of DMSO

As a solvent, dimethyl sulfoxide (DMSO) was used in the control group to dissolve 6-Gingerol[15]. It is acknowledged that DMSO, particularly at higher concentrations, is known to possess minor free-radical scavenging properties and may exert some effects on cell membrane fluidity[10]. However, our study included a dedicated DMSO control group (Group DMSO) which received the same volume of the solvent as the 6G-IR group. Critically, the DMSO group showed no significant difference from the Sham group across all measured parameters (deformability, MDA, SOD, and eNOS H-score). Therefore, we conclude that the biological effects observed in the 6G-IR group are attributable solely to 6-Gingerol, and any potential confounding effect of the DMSO solvent was negligible at the concentration and administration route used. Although a DMSO + IR group was not included, the absence of any detectable effect of DMSO alone across all endpoints suggests that its contribution under IR conditions would be negligible.

In summary, this study provides compelling evidence that 6-Gingerol protects against IR-induced erythrocyte dysfunction. The dual action of enhancing SOD-mediated superoxide neutralization while concomitantly reducing membrane lipid peroxidation (MDA) provides a clear mechanistic rationale for the observed preservation of erythrocyte deformability and morphology.

Conclusions

In conclusion, this study provides strong evidence that prophylactic treatment with 6-Gingerol significantly protects against erythrocyte dysfunction induced by skeletal muscle ischemia-reperfusion (IR) injury in a rat model. This protective effect is achieved primarily through the robust enhancement of antioxidant capacity, specifically Superoxide Dismutase (SOD) activity, which successfully minimizes lipid peroxidation (MDA levels) and preserves the viscoelastic properties of the erythrocyte membrane. These findings not only validate the antioxidant potential of 6-Gingerol but, more importantly, offer a novel mechanistic insight by demonstrating that preserving erythrocyte deformability is a key component of its overall protective mechanism against IR

injury. Further research is warranted to explore its clinical application as a rheological modulator in conditions involving microvascular compromise.

Limitations

The current study is subject to several limitations. First, the study relies on a single time point of analysis (90 min of reperfusion), which may not fully capture the dynamic nature of IR injury progression or the long-term efficacy of 6-Gingerol. Second, while our findings strongly suggest a mechanism involving the neutralization of superoxide and the prevention of peroxynitrite formation, we did not directly measure functional nitric oxide bioavailability (e.g., nitrite/nitrate levels) or specific peroxynitrite markers (e.g., nitrotyrosine) to definitively confirm the eNOS related mechanism. Third, the study was conducted on a localized skeletal muscle IR model; therefore, the results may not be directly generalizable to systemic or different organ IR models. Fourth, the exclusive use of male rats in this study may limit the generalizability of our findings due to known sex-based differences in oxidative stress response and cardiovascular dynamics. Finally, the Resource Equation Method was utilized for sample size determination, which is appropriate for exploratory studies, but subsequent larger studies using power calculations based on our observed effect sizes are needed to confirm the findings robustly.

Data availability

The dataset is available on request from the authors. Please contact the MD. Tuna DEMİRKIRAN (tuna.demirkiran@sbu.edu.tr) for data access inquiries.

Received: 6 May 2025; Accepted: 12 January 2026
Published online: 18 January 2026

References

1. Granger, D. N. & Kvietys, P. R. Reperfusion injury and reactive oxygen species: the evolution of a concept. *Redox Biol.* **6**, 524–551 (2015).
2. Catalá, A. Lipid peroxidation of membrane phospholipids generates hydroxy-alkenals and oxidized phospholipids active in physiological and/or pathological conditions. *Chem. Phys. Lipids*. **157**, 1–11 (2009).
3. Pretorius, E. Erythrocyte deformability and eryptosis during inflammation, and impaired blood rheology. *Clin. Hemorheol Microcirc*. **69**, 545–550 (2018).
4. Ebenuwa, I. et al. Altered RBC deformability in diabetes: clinical characteristics and RBC pathophysiology. *Cardiovasc. Diabetol.* **23**, 370 (2024).
5. Zheng, Y. et al. Characterization of red blood cell deformability change during blood storage. *Lab. Chip*. **14**, 577–583 (2014).
6. Tai, Y. H. et al. Vitamin C supplementation attenuates oxidative stress and improves erythrocyte deformability in cardiac surgery with cardiopulmonary bypass. *Chin. J. Physiol.* **65**, 241–249 (2022).
7. Mashhadi, N. S. et al. Anti-oxidative and anti-inflammatory effects of ginger in health and physical activity: review of current evidence. *Int. J. Prev. Med.* **4** (Suppl 1), 36–42 (2013).
8. Pázmándi, K., Szöllősi, A. G. & Fekete, T. The root causes behind the anti-inflammatory actions of ginger compounds in immune cells. *Front. Immunol.* **15**, 1400956 (2024).
9. Mead, R., Gilmour, S. G. & Mead, A. *Statistical Principles for the Design of Experiments: Applications To Real Experiments* (Cambridge University Press, 2012).
10. Kelava, T., Ćavar, I. & Čulo, F. Biological actions of drug solvents. *Period Biol.* **113**, 311–320 (2011).
11. Lv, X. et al. 6-gingerol activates PI3K/Akt and inhibits apoptosis to attenuate myocardial ischemia/reperfusion injury. *Evid. -Based Complement. Altern. Med.* (2018).
12. Xu, T. et al. 6-gingerol protects heart by suppressing myocardial ischemia/reperfusion induced inflammation via the PI3K/Akt-dependent mechanism in rats. *Evid. -Based Complement. Altern. Med.* (2018).
13. Kongsui, R. & Jittiwat, J. In vivo protective effects of 6-gingerol in cerebral ischemia involve preservation of antioxidant defenses and activation of anti-apoptotic pathways. *Biomed. Rep.* **20**, 85 (2024).
14. Cayman Chemical. *Product Information, 6-Gingerol, Item No 11707*. https://cdn.caymanchem.com/cdn/insert/11707.pdf (2024).
15. Kartal, H. & Comu, F. M. Effect of melatonin on erythrocyte deformability in mice with Ischemia-Reperfusion injury in skeletal muscle. *J. Surg. Res.* **3**, 262– (2020).
16. Arslan, M., Comu, F. M., Isik, B., Unal, Y. & Cekmen, N. Kurtipek, O. Effects of the general anaesthetic agent, propofol, on erythrocyte deformability. *Bratisl Lek Listy*. **111**, 126–128 (2010).
17. Široká, M. et al. Nuclear factor-kB and nitric oxide synthases in red blood cells: good or bad in obesity? A preliminary study. *Eur. J. Histochem*. **64**, 3081 (2020).
18. Kleinbongard, P. et al. Red blood cells express a functional endothelial nitric oxide synthase. *Blood* **107**, 2943–2951 (2006).
19. Leo, F. et al. Red blood cell and endothelial eNOS independently regulate Circulating nitric oxide metabolites and blood pressure. *Circulation* **144**, 870–889 (2021).
20. Fischer, T. M. Shape memory of human red blood cells. *Biophys. J.* **86**, 3304–3313 (2004).
21. Grisham, M. B. & Granger, D. N. Free radicals: reactive metabolites of oxygen as mediators of postischemic reperfusion injury. *In Splanchnic Ischemia and Multiple Organ Failure*. 135–144. (Mosby: St. Louis, 1989).
22. Zhang, M., Fangfang, P., Zhang, R., Zhao, L. & Wu, Y. The antioxidant effect of Picroside II and the optimizing of therapeutic dose and time window in cerebral ischemic injury in rats. *Merit Res. J. Pharm. Pharm. Sci.* **1**, 1–7 (2013).
23. Radi, R., Beckman, J. S., Bush, K. M. & Freeman, B. A. Peroxynitrite-induced membrane lipid peroxidation: the cytotoxic potential of superoxide and nitric oxide. *Arch. Biochem. Biophys.* **288**, 481–487 (1991).
24. Girotti, A. W. Nitric oxide-elicited resistance to antitumor photodynamic therapy via Inhibition of membrane free radical-mediated lipid peroxidation. *Photochem. Photobiol.* **97**, 653–663 (2021).
25. Subramani, J., Kundumani-Sridharan, V. & Das, K. C. Chaperone-mediated autophagy of eNOS in myocardial ischemia-reperfusion injury. *Circ. Res.* **129**, 930–945 (2021).
26. Zhao, H., Zhang, R., Yan, X. & Fan, K. Superoxide dismutase nanozymes: an emerging star for anti-oxidation. *J. Mater. Chem. B.* **9**, 6939–6957 (2021).
27. Winterbourn, C. C., Gutteridge, J. M. & Halliwell, B. Doxorubicin-dependent lipid peroxidation at low partial pressures of O2. *J. Free Radic Biol. Med.* **1**, 43–49 (1985).

Author contributions

**Conceptualization: ** T.Ö. and T.D.; **Methodology: ** H.K., E.D., Ş.K., and I.Ö.; **Software: ** E.E.; **Vali-

dation: ** E.E., M.E.Ö., and B.Y.; **Formal analysis: ** E.E. and G.E.; **Investigation: ** T.Ö., H.K., F.M.Ç., E.D., B.Y., G.E., T.D., M.E.Ö., I.Ö., Y.T., and V.C.Ö.; **Resources: ** Y.T. and V.C.Ö.; **Data curation: ** F.M.Ç. and B.Y.; **Writing—Original draft preparation: ** T.Ö., H.K., and T.D.; **Writing—Review and editing: ** T.Ö., H.K., E.D., G.E., and T.D.; **Visualization: ** Y.T.; **Supervision: ** H.K. and E.D.; **Project administration: ** V.C.Ö.; **Funding acquisition: ** Y.T. All authors have read and agreed to the published version of the manuscript.

Declarations

Competing interests
The authors declare no competing interests.

Additional information
Correspondence and requests for materials should be addressed to T.Ö.

Reprints and permissions information is available at www.nature.com/reprints.

Publisher's note Springer Nature remains neutral with regard to jurisdictional claims in published maps and institutional affiliations.